

Influence of existing building load on the deformation and earth pressure of ground due to tunneling

Influence de la charge de bâtiments existants sur la déformation et la pression des terres d'un sol en tunnelage

T. Nakai, H.M. Shahin, M. Hinokio, T. Sada & E. Sung
Department of Civil Engineering, Nagoya Institute of Technology, Nagoya, Japan

ABSTRACT

To investigate the influence of existing building load on the deformation and earth pressure of the ground in shallow tunneling, two-dimensional trap-door model tests and the corresponding numerical analyses are carried out. A stack of aluminum rods is used in the model tests. Shallow and pile foundations supporting an initial dead load are modeled in the laboratory tests and numerical analyses. For the sake of comparison the laboratory tests and numerical simulations for tunneling in the initially undisturbed ground condition (i.e., green field) are performed as well. In the finite element analyses, a recently developed elastoplastic constitutive model, named subloading t_{ij} model, is used. The observed and computed results for the ground with existing building load are compared with those for the green field condition.

RESUME

Pour étudier l'influence de la charge de bâtiments existants sur la déformation et la pression des terres d'un sol en tunnelage à faible profondeur, plusieurs essais de modèles de trappes en deux dimensions ont été réalisés avec leurs analyses numériques respectives. Une pile de barres d'aluminium est utilisée dans les essais de modèles. Le fond et les fondations sur pieux soutenant une charge morte, simulant les bâtiments existants, sont modélisés dans les essais en laboratoire ainsi que dans les analyses numériques. A titre de comparaison, des essais en laboratoire et les simulations numériques correspondantes d'une excavation d'un sol non chargé initialement (i.e. en conditions d'espace vert) ont également été effectués. Pour les analyses par éléments finis, a été utilisé un modèle de comportement élastoplastique développé récemment, le "subloading t_{ij} model". Les résultats observés et calculés pour le sol chargé de bâtiments existants sont ainsi comparés à ceux correspondants aux conditions d'espace vert.

1 INTRODUCTION

It is essential to utilize the underground space efficiently in urban redevelopment. However, due to the interference of existing buildings and several other factors, sometimes cut and cover method is not possible in urban area. In these cases, advanced tunneling methods, which cause less damage to the existing buildings, are necessary. In the practical design of tunnels, the earth pressure is evaluated based on classical rigid plastic theory, and the ground movement, including surface settlement, is estimated by elastic analysis or empirical methods. These methods are not consistent from the mechanical viewpoint, and cannot consider properly the influence of construction sequence and existing building loads on the ground movement and earth pressure.

To investigate the influence of the construction sequence and footing loads of existing building in tunneling, 2D and 3D model tests and the corresponding numerical analyses were carried out (Shahin et al., 2004(a) and 2004(b)). The results of these researches show that 3D effects and the existing building loads have a significant influence on the surface settlements and earth pressure in the ground, and that finite element analysis in which typical soil properties are precisely taken into account can simulate such influences properly. In the present paper, model tests and numerical analyses were conducted in order to investigate the effect of tunneling on the surface settlement and the earth pressure of the ground and the subsidence of an existing building with either footing or pile foundations.

2 OUTLINE OF THE ELASTOPLASTIC MODEL USED IN THE ANALYSES

The subloading t_{ij} model is used in the numerical analyses. This model, despite the use of a small number of material parameters,

can describe properly the following typical features of soil behavior:

- (1) Influence of intermediate principal stress on the deformation and strength of soils.
- (2) Dependence of the direction of plastic flow on the stress paths.
- (3) Influence of density and/or confining pressure on the deformation and strength of soils.

Defining a yield function with modified stress t_{ij} and considering associated flow rule in t_{ij} -space instead of σ_{ij} -space, feature (1) is obtained. Dividing plastic strain increment into two components for the same yield function, this model can take into consideration feature (2). Referring to the subloading surface concept proposed by Hashiguchi (1980) and revising it, feature (3) is considered. The details of this model have been described in the paper by Nakai & Hinokio (2004).

Figure 1 shows the test results (dots) and the corresponding calculated simulations (solid curves) of biaxial tests on samples made of aluminum rods, having diameters of 1.6 and 3.0mm and mixed in a ratio of 3:2 in weight, under constant major principal stress ($\sigma_1=19.6\text{kPa}$) and minor principal stress ($\sigma_2=19.6\text{kPa}$). It is seen that the strength and deformation behavior is very close to that of dense sand. The dotted curves in these figures represent the calculated results for a confining pressure of 1/100 times the confining pressure of the experiments. It can be seen that this model can express the dependency of stiffness, strength and dilatancy on the density as well as on the confining pressure. Material parameters for the aluminum rod mass are shown in the Table 1. These parameters are independent of the ground density and the confining pressure.

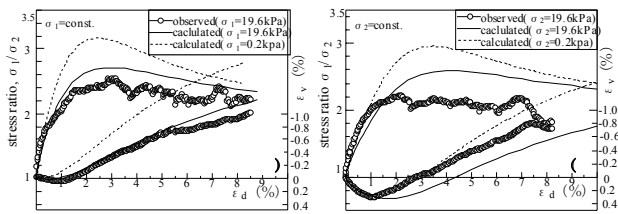


Figure 1. Stress-strain-dilatancy curve of aluminum rods mass

Table 1. Parameters of soil materials

Parameters	Value
λ	0.0080
κ	0.0040
N (e_{NC} at $p=98kPa$ & $q=0kPa$)	0.30
$R_{CS}=(\sigma_1/\sigma_3)_{CS(comp.)}$	1.80
β	1.20
v_c	0.20
a	1300

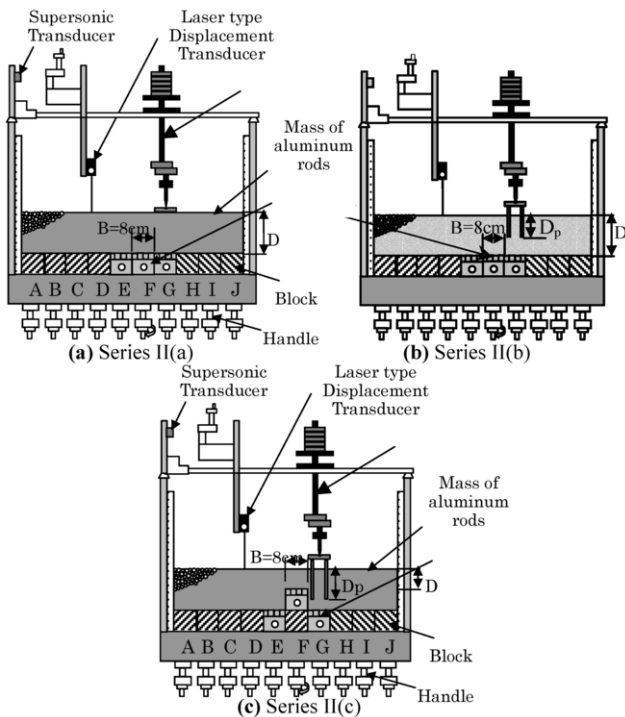


Figure 2. Trap door apparatus

3 DESCRIPTION OF MODEL TESTS AND ANALYSES

It is intended to simulate tunneling along a road adjacent to an existing building with footing or pile foundations, as it is usual in real cases. Two dimensional model tests are carried out to investigate the basic mechanism of the ground behavior and earth pressure for a tunnel excavation. Figure 2(a) shows the 2D trap door apparatus for footing foundation, and Figures 2(b) and (c) show those for pile foundations. The length of pile D_p in Figure 2(b) is shorter than the depth of the top of the lowering block, which simulates the tunnel roof. The whole apparatus consists of 10 brass blocks (blocks A to J) of 8cm in width each, placed along the centerline of an iron table. Ground is made with the mass of aluminum rods as described above. The unit weight of the aluminum rod mass is $20.4kN/m^3$. Initial condition of the model tests is set up by placing the footing on the ground or installing the piles in the ground, and applying the dead load at

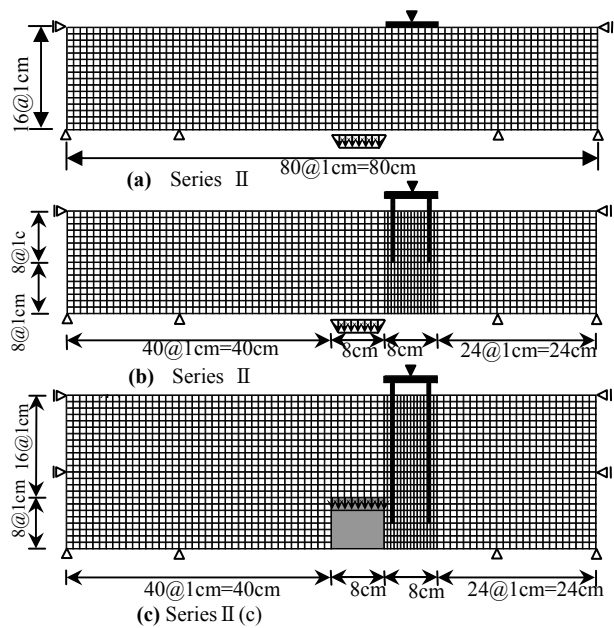


Figure 3. Finite element meshes ($D/B=2.0$)

the top of footing or piles as shown in the figures. Tunnel excavation is simulated by imposing a vertical downward displacement of 4mm to block F. In every excavation step, earth pressure is measured in 3 blocks, each of which contains of 4 load cells. The surface settlement is measured using a laser type displacement transducer. By taking photos of the ground with a digital camera, the deformation patterns of the ground can also be visualized. Details of the apparatus and test procedure can be found in Shahin et al. (2004-a).

Table 2 shows the patterns of the model tests and analyses. Series I is for the case without building load (green field), Series II(a) is for the case with footing (see Figure 2(a)), Series II(b) is for the case with piles whose length D_p is shorter than the tunnel depth D (see Figure 2(b)), and Series II(c) is for the case with longer piles where the pile length is longer than the tunnel depth (see Figure 2(c)). The model footing is made of an aluminum plate of 8cm in length and 2cm in thickness. The pile is made of polyurethane plates of 5mm in thickness, and its bending stiffness EI is $101.3N \cdot cm^2$. The pile material is chosen assuming a similarity ratio of 1:100 between the model test and the prototype in which concrete piles of 1m in diameter are arranged at intervals of 5.5m.

Table 2. Patterns of tunnel excavation

condition	D/B		
Series I	1.0	2.0	3.0
Series II(a)	1.0	2.0	3.0
Series II(b)		2.0	
Series II(c)	1.0	2.0	

Numerical analyses are conducted for the same scale of the model tests considering plane strain drained conditions. Figures 3(a) to (c) show the meshes for the grounds corresponding to the model tests in Figures 2(a) to (c), respectively. Both vertical faces of the mesh are free in the vertical direction and the bottom face is kept fixed. To simulate the lowering of the blocks, vertical displacements are imposed at the nodal points, which correspond to the top of the lowering blocks in the model tests. Friction behavior between soil and structure is simulated using an elastoplastic joint element (Nakai, 1985). The surface friction angles of the footing and piles are determined experimentally as 15° and 17° , respectively. The initial ground condition in every analysis is obtained by imposing body forces ($\gamma=20.4kN/m^3$) to

all elements under one-dimensional strain condition, starting from a negligible confining pressure ($p_0=9.8 \times 10^{-6}$ kPa) and an initial void ratio of $e=0.35$.

4 RESULTS AND DISCUSSIONS

4.1 Influence of loads with footing

Figures 4(a) and (b) show the observed and computed surface settlements of Series II(a), together with the results of Series I (green field) in case of $D/B=1.0$, 2.0 and 3.0. In these figures, open dots denote the results for Series II, and solid dots for Series I. The position of the applied dead load is depicted at the top in each figure. The applied load ($Q_v=0.32 \times 9.8$ N/cm) is approximately one third of the ultimate bearing capacity load. From the model test results, it is seen that due to the existing load, the maximum surface settlement is offset towards the position of the dead load, and it is larger than that for the green field condition. The plate of the dead load tilts towards the excavation except for $D/B=3.0$. In this case a little tilt was observed in the opposite direction. The maximum tilting was observed for $D/B=1.0$. The computed surface settlement and settlement trough are almost same as those in the model tests, except for a little difference in the magnitude of surface settlement in case of $D/B=1.0$. Figures 5(a) and (b) show the observed movement (photo) and the computed displacement vectors in the model ground for $D/B=2.0$. The observed movement is obtained by superimposing two photos – before and after lowering the block. It is revealed in this figure that the deformed zone spreads towards the loaded plate from the top of the lowering block. The computed displacement vectors show the same tendency as the model test.

Figures 6(a) and (b) show the earth pressure distributions of the model tests and numerical analyses, respectively. The left vertical axis represents the earth pressures normalized by the initial earth pressure $\sigma_z=\gamma D$, and the right vertical axis represents the actual values of earth pressure in Pascal. Legends indicate the amount of applied displacement. Here, the dotted curves with black circular marks represent the earth pressures before applying building loads, while the white circular marks show the pressures after applying building loads. Irrespective of the ground depth, a significant amount of load transfer from the tunnel roof to the adjacent zones on both sides is observed due to ground arching. This effect is more remarkable on the side where the building load is applied. The observed earth pressure at the place of excavation decreases suddenly with a little displacement (less than 1mm) of the lowering block, and after that it becomes almost constant, irrespective of the imposed displacement. It is also noticed that the earth pressure at the lowering block is asymmetric and is independent of the depth. The results of the numerical analyses capture well the results of the model tests both in shape and quantity.

Figures 7 and 8 show the observed and computed surface settlement profiles and ground movements for $D/B=2.0$, when larger surface load ($Q_v=0.56 \times 9.8$ N/cm) is applied. As can be seen from Figure 9 which is the computed load-settlement curves of the footing, the load level in this case is slightly lower than the residual strength of the ground. The surface heaves above the tunnel and on the other side of the loaded plate. Deformation zone of the ground spreads towards the loaded plate as before, but from this point a sliding rotational mechanism spreads towards the left at the excavation side. Due to the excessive shearing of the ground in the left side and beneath the loaded plate, it tilts in the opposite direction of tunnel excavation in a pattern which is different from that in Figure 4 ($Q_v=0.32 \times 9.8$ N/cm). These results show that the ground movement due to tunneling varies with the magnitude of the building loads as well. The numerical analyses can accurately predict the results of the model tests.

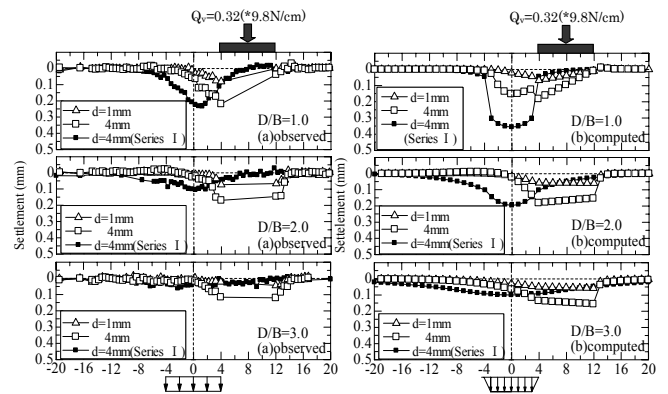


Figure 4. Profiles of surface settlement: Series II (a)

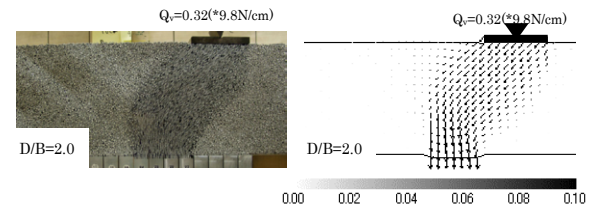


Figure 5. Ground movement: Series II (a)

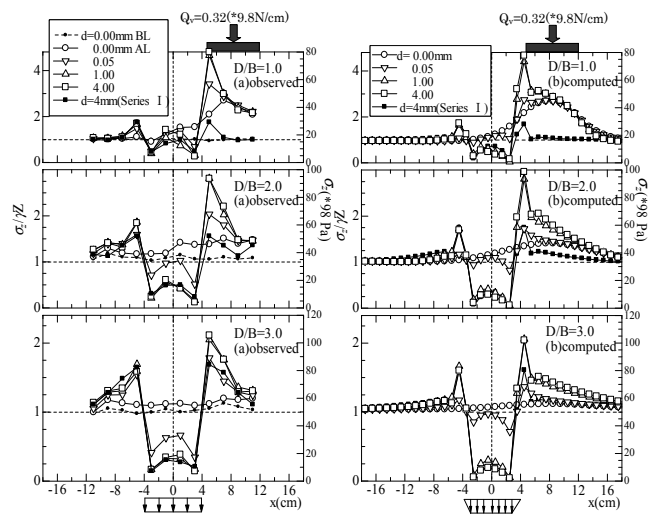


Figure 6. Earth pressure distribution: Series II (a)

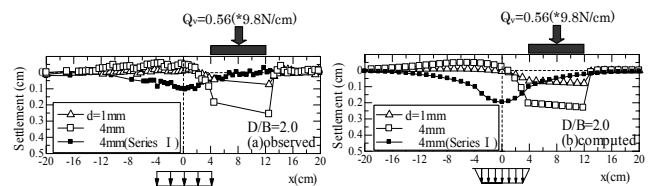


Figure 7. Profiles of surface settlement: Series II (a) (existing load = 0.56×9.8 N/cm)

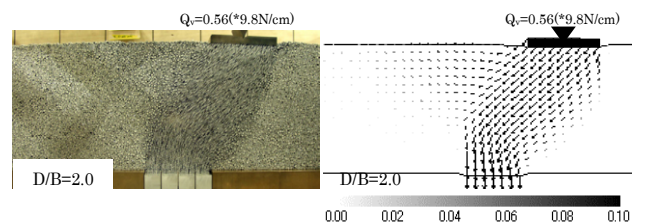


Figure 8. Ground movement: Series II (a) (existing load = 0.56×9.8 N/cm)

4.2 Influence of loads with piles

Figures 10 and 11 show the observed and computed surface settlement profiles and ground movements for $D/B=2.0$ and $D_p/B=1.0$ in Series II(b), when total pile load $Q_v=0.32*9.8\text{N/cm}$ is applied at the top of piles. The results for the green field (Series I) are also indicated by solid dots in Figure 10. The arrows at the top of Figure 10 indicate the position of the piles. Maximum surface settlement occurs not above the lowering block but at the position of foundation in the same way as that in Figure 4 (footing), and the profile of the settlement is similar not to that for $D/B=2.0$ but to that for $D/B=1.0$ in Figure 4. It is also seen from Figure 11 that the deformed zone develops asymmetrically toward the front pile, though the trend is not so remarkable as that in Figure 5. It is seen from Figure 12 that the observed and computed vertical earth pressure distributions at the depth of the top of lowering block show the same tendency as those with footing in Figure 6.

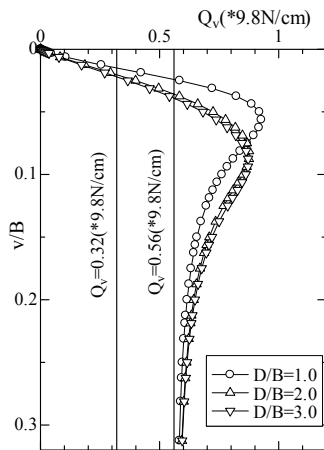


Figure 9. Computed load-settlement curve of footing

Figures 13 and 14 show the observed and computed profiles of the surface settlements and ground movement for the case of Series II(c), in which the length of the piles D_p is longer than the depth of the top of the lowering block. The results for two cases are indicated – one is the case of $D/B=1.0$ and $D_p/B=1.5$, and the other is the case of $D/B=2.0$ and $D_p/B=2.5$. When the length of the piles is longer than the tunnel depth, the settlement of the foundation is restrained, though the surface settlement above the tunnel and on the other side of the foundation becomes larger than that for the green field. As can be seen from Figure 14, the deformed zone becomes smaller at the side of the foundation, but spreads wider at the opposite side. The model test and numerical analysis for the piles (longer than the soil cover) without existing load were also carried out. The profile of the surface settlement is similar to those in Figure 13 (The result is omitted here). Therefore, to prevent the severe subsidence of an existing building, it is effective to install sheet piles deeper than the tunnel between the building and tunnel.

5 CONCLUSIONS

Through the experimental and numerical studies, it is shown that the existing building load influences very much on the subsidence of the building, as well as on the surface settlement and earth pressure due to tunneling. The magnitude and the pattern of the settlement are controlled not only by the type of the foundation but also by the magnitude of the building load. The computed results in which typical stress-strain behavior of soils is appropriately taken into account agree well with the experimental results qualitatively and quantitatively.

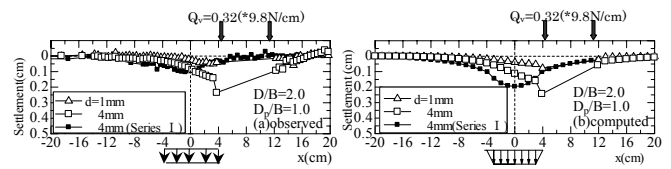


Figure 10. Profiles of surface settlement: Series II (b)

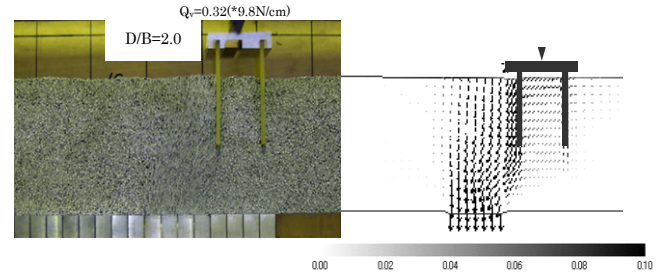


Figure 11. Ground movement: Series II (b)

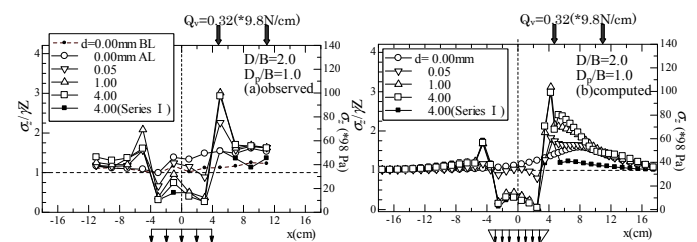


Figure 12. Earth pressure distribution: Series II (b)

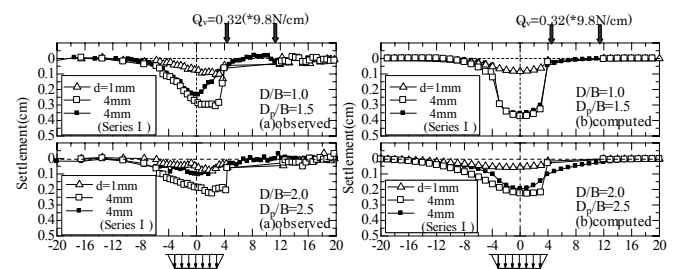


Figure 13. Profiles of surface settlement: Series II (c)

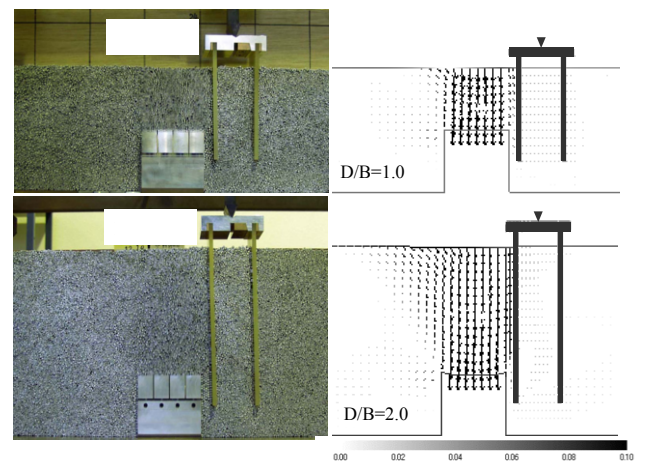


Figure 14. Ground movement: Series II (c)

REFERENCES

- Hashiguchi, K. 1980. Constitutive equation of elastoplastic materials with elasto-plastic transition. *Jour. of Appli. Mech.*, ASME, 102(2), 266-272.
- Nakai, T. 1985. Finite element computations for active and passive earth pressure problems of retaining wall. *Soils and Foundations*, 25(3), 98-112.
- Nakai, T. and Hinokio, M. 2004. A simple elastoplastic model for normally and over consolidated soils with unified material parameters. *Soils and Foundations*. 44(2), 53-70.
- Shahin H. M., Nakai, T., Hinokio, M., Kurimoto, T. and Sada, T. 2004. Influence of surface loads and construction sequence on ground response due to tunneling. *Soils and Foundations*, 44(2), 71-84.
- Shahin, H. M., Nakai, T., Hinokio, M. and Yamaguchi, D. 2004. 3D effects on earth pressure and displacements during tunnel excavations. *Soils and Foundations*, 44(5), 37-49.